

GOESR3 Periodic Reporting

Reporting Period: July 2019 – Dec 2019 (1st half of FY19 funding cycle)

Team Lead: Xuguang Wang (PI, OU)

Team Members: co-PIs Aaron Johnson (OU), Thomas Jones (OU), Jason Otkin (WI), Yanqiu Zhu (EMC)

Project Title: Assimilation of high resolution GOES-R ABI infrared water vapor and cloud sensitive radiances using the GSI-based hybrid ensemble-variational data assimilation system to improve convection initiation forecast.

Project Number: NA16OAR4320115

Executive Summary

The primary objectives of the project include (a) further extend the GSI EnKF/EnVar DA system for assimilating high resolution GOES-R ABI infrared water vapor and cloud sensitive radiance observations by ingesting convection resolving model's own high-resolution EnKF ensemble rather than the GFS ensemble and by directly updating cloud hydrometeor variables; (b) improve the usage of GOES-R ABI water vapor and cloud sensitive radiances for rapidly updated DA by refining data quality control, using high-resolution infrared land surface emissivity databases and exploring all-sky bias correction and observation error methods, and (c) test different DA configurations and evaluate the impact of assimilating GOES-R water vapor and cloud sensitive radiance observations for the prediction of diverse CI events when combined with ground based observation networks.

During this reporting period, progress was focused on three main research questions:

- A) Can a simple additive noise technique provide improved direct all-sky IR radiance assimilation in GSI-EnKF during the rapid initiation of supercell in a case study?
- B) Does adaptive observation error inflation improve the relative weight given to ABI and radar observations during DA in a way that improve forecasts, and what can we learn about the relative strengths and limitations contributed by the different observation datasets (radar, channel 9 and channel 10) after implementing these techniques and optimizations in the GSI-EnKF?
- C) Do the theoretical differences between offline and online bias correction technique still apply in the real-world context of bias correcting ABI radiances with radar reflectivity as an anchor observation?

Progress toward FY19 Milestones

The project progresses as planned in general. Progress during this reporting period have led to a better understanding of the important issues for bias correction of all-sky IR radiance in the context of CI forecasts.

Specific progresses are described below.

A) ADDITIVE NOISE IMPLEMENTATION FOR RADIANCE ASSIMILATION

Our previously reported experiment that assimilates channel 10 radiance and radar reflectivity is able to initialize the northern storm well by 1830 UTC, but the southern storm is still missing from this experiment (Fig. 1; top row). The inability to initialize the southern storm, even when assimilating both radar reflectivity and ABI radiance, results from the storm being missing from all ensemble members in the background forecasts. Thus, the ensemble covariance between the observation departures and model variables related to storm development are zero. To solve this, we adopt the additive noise technique that is commonly used in radar reflectivity data assimilation.

Additive noise is newly implemented in the GSI-EnKF system for all-sky ABI radiance assimilation. The first step of the additive noise is to identify clear and cloudy pixels in a consistent way for both the observations and the model priors. We adopt the technique of Harnisch et al. (2016) for determining a brightness temperature (BT) threshold that distinguishes clear and cloudy pixels in a given channel with a low mis-classification rate (not shown). The resulting BT thresholds are 239 K for channel 9 and 251 K for channel 10. These thresholds are used to identify pixels where the observations are cloudy and the ensemble mean background is clear. At these locations, random noise with a standard deviation of 0.25 K, 0.25 K, and 0.25 m/s is applied to each members' temperature, dew point and wind variables at that location, below 500 hPa, with a de-correlation scale for the noise of 12 km in the horizontal and 3 km in the vertical directions.

After implementing the additive noise in the channel 10 experiment, the northern storm is well initialized two cycles earlier and the southern storm is able to be initialized in the 1830 cycle (Fig. 1; middle row). The reason for the improvement can be further understood via the cross section of model increments along the black line from figure 1 during the 1820 and 1830 UTC DA cycle (Fig. 2). After adding additive noise, much deeper increments to temperature, moisture and cloud hydrometeors are added to the analysis in the 1820 UTC cycle near cells 1 and 3. However, significant deep increments in the vicinity of the southern cell 2 are not seen until the 1830 UTC cycle. Although this cross-section does not necessarily capture the full horizontal structure of the increments, even the increment at 1830 UTC in cell 2 shows more cooling than we would expect to see when we should be adding a positively buoyant storm updraft. As discussed further in the following section, this suggests that the correct background ensemble covariance structure associated with initiating convection is taking several cycles to spin up even with the newly implemented additive noise, causing the relatively delayed initialization of the southern storm.

B) ADAPTIVE OBSERVATION ERROR FOR RADIANCE ASSIMILATION

We noticed in the experiment described above (assimilating channel 10 radiance and radar reflectivity with additive noise) that the low level moisture increment corresponding to the southern storm was displaced ~10km east of the observed storm cell, which should be aligned with the location of the cross-section line (Fig. 3). The displacement results from the tilted storm structure, whereby the coldest cloud tops in the storm anvil are displaced east of the low level storm updraft. Since the observation error of 1 K (5 dbz) for radiance (reflectivity) in this experiment is at the low (high) end of what other studies have

used, we hypothesized that too much weight was being given to the vertical correlation to the radiance observation of cloud top rather than the low level information provided by the reflectivity observations. Since the proper background error covariance structure is still spinning up at this time, this is likely a suboptimal way to combine the information from the radar reflectivity and channel 10 ABI radiance observations in the DA system.

In order to alleviate this issue, we adopt the method for determining observation error as a function of symmetric cloud effect from Harnisch et al. (2016). In short, the method consists of defining a cloud impact on forecast radiance and cloud impact on observed radiance as $C_f = \max[0, BT_{lim} - BT_f]$ and $C_o = \max[0, BT_{lim} - (BT_o - bias)]$, respectively, and define the symmetric cloud impact $C = (C_f + C_o)/2$. We then use one of our earlier experiments to calculate the average Root Mean Square Innovation (RMSI) as a function of C for different ABI radiance channels. Since we know $RMSI = \sqrt{s_o^2 + s_f^2}$, and assume that the forecast uncertainty is well sampled by the ensemble spread, s_f^2 , we can calculate an estimate of the observation uncertainty, s_o^2 , as a function of C (Fig. 4).

The impact of implementing this adaptive observation error technique in the channel 10 DA experiment is to both improve the forecasts of the reflectivity swath (Fig. 1; bottom row) and updraft helicity swath (Fig. 5). The improvement is a result of the more coherent analysis and forecast storm structure when more weight is given to the radar reflectivity during DA to constrain the lower levels of the storms. Similar experiments have also been run with ABI channel 9 and with channel 9 and channel 10 assimilated together (Table 1). Ongoing work is using various diagnostics, including the DA increments in both observation and model space, to evaluate the strengths and limitations of assimilating the different observation datasets (radar, channel 9 and channel 10) in the context of the newly improved GSI-EnKF DA system with all-sky IR radiances. Preliminary investigation of the structure of the ensemble background error covariances in these experiments suggests that (a) development of a static storm initiation covariance model is needed to improve the additive noise implementation for ABI radiances, and (b) channel 9 radiances has some advantage of channel 9 radiances during the initiation period of rapidly developing convection because of a greater ensemble spread in observation space. These results, and those described above, are currently being prepared for submission Monthly Weather Review.

C) OPTIMIZING BIAS CORRECTION FOR CYCLED CONVECTIVE SCALE ASSIMILATION OF ABI

In the last report, the effect of non-linear bias correction with two different predictors, namely observed and simulated brightness temperature (BT) predictor, was shown. It was seen that simulated BT predictor adds more clouds in the analysis, thereby creating cold BTs at the storm location compared to the analysis from the observation BT predictor experiment. In this report period, major focus was given to the comparison of the offline and online method of bias correction.

The non-linear bias correction we implemented in previous reports is an offline bias correction procedure. In the mean time GSI-EnKF has an online iterative bias correction procedure. In order to understand the difference between these two methods, the iterative GSI-EnKF bias correction was modified (i.e. the form of predictors were modified in order to be consistent with the offline non-linear bias correction procedure). This way both the offline and online method uses a cubic polynomial form for bias correction. After the above modifications, default iterative bias correction coefficients were cycled in order to get converged bias coefficients. Figure 6a and 6b shows the observation-minus-analysis contours

at different DA times from 1710 to 1830 UTC. It is evident that the online bias correction experiment results in a more accurate analysis compared to the offline bias correction experiment. It is interesting to note that both the online and offline bias correction has not produced cold BT in the analysis corresponding to the storm location.

The domain average background RMSE in brightness temperature for different DA cycles shown in figure 7 also portrays the better performance of online bias correction compared to offline. With the above results, the next logical step would be to explore the theoretical difference between the two bias correction schemes. Eyre (2016) uses a simple model to explain the difference between online and offline method of bias correction. Some of the assumptions made in the simple model are (i) the bias is considered as a global offset value without any spatial variation and (ii) both the bias corrected and anchor observation are observing the same quantity. It was shown that in the presence of model bias, the analysis/background bias when using an online bias correction, tend to represent a less fraction of model bias compared to the offline bias correction. The existing online and offline approach of bias correction of ABI radiances, express the bias as a function of predictor. Furthermore, the observations used in the DA system are of two different types, namely RADAR and RADIANCE, which are sensitive to different quantities. Also, the RADAR observations are not able to act as anchor observations in the clear-sky regions whereas in the cloudy/spurious cloud regions they can anchor the analysis. Owing to these differences, the conclusions from Eyre (2016) cannot be extended to the current experiment results. The research question we would like to ask is “With the similar assumptions made in Eyre(2016), can we validate the conclusions on offline and online bias correction in a realistic DA system?”. In order to extend the conclusions from Eyre (2016) to realistic DA system, modifications have been made to the existing system. With these modifications, experiments are being run using both offline and online bias correction experiments along with the diagnostics in RADAR reflectivity space.

Plans for Next Reporting Period

Continued analysis of the already-conducted experiments summarized by Table 1 is ongoing into the next reporting period. This includes detailed examination of the increments in both observation and model space, as well as investigation of the ensemble background error covariance to understand why we see such increments and how to optimally combine the radar, channel 9, and channel 10 ABI observations in the DA system. An additional experiment updating the additive noise to have random draws from a pre-defined static covariance model appropriate for initiating deep convection may also be explored down the road.

For the next reporting period, the modified bias correction experiments to show the difference between offline and online bias correction will be conducted along with detailed diagnostics. The diagnostics will include quantifying the model, analysis and background bias by looking at the RADAR reflectivity space for both offline and online bias correction experiments. The goal of these experiments is to determine whether the theoretical difference between offline and online bias correction method as outlined in Eyre (2016) holds well for realistic convective scale DA system.

Additional Information

1. Interaction with operational partners –

The proposing team interacted with NCEP/EMC collaborator Yanqiu Zhu during the extension and testing of the GSI EnKF system with the ABI clear air and cloudy radiance assimilation including pre-processing, QC, code modifications. The proposing team also interacts with NCEP/EMC collaborator Ming Chen on the implementation of high resolution surface emissivity with CRTM-CSEM

2. Conference/workshop participation –

We continue participating the bi-weekly GSI developers meeting hosted by NCEP/EMC.

Wang, X., A. Johnson and K. Chandramouli, Thomas Jones, Jason Otkins, Jeff Whitaker, 2020: A Comparison of Different Bias Correction Methods on the Assimilation of High-Resolution All-Sky *GOES-16* ABI Radiances to Improve Convective Initiation Forecasts. AMS annual meeting, Boston

2. Outside project publicity –

N/A during this project period.

4. Journal articles –

N/A during this project period as the primary effort is system development and diagnostics. Papers including scientific results will be submitted in the future.

Key Graphics

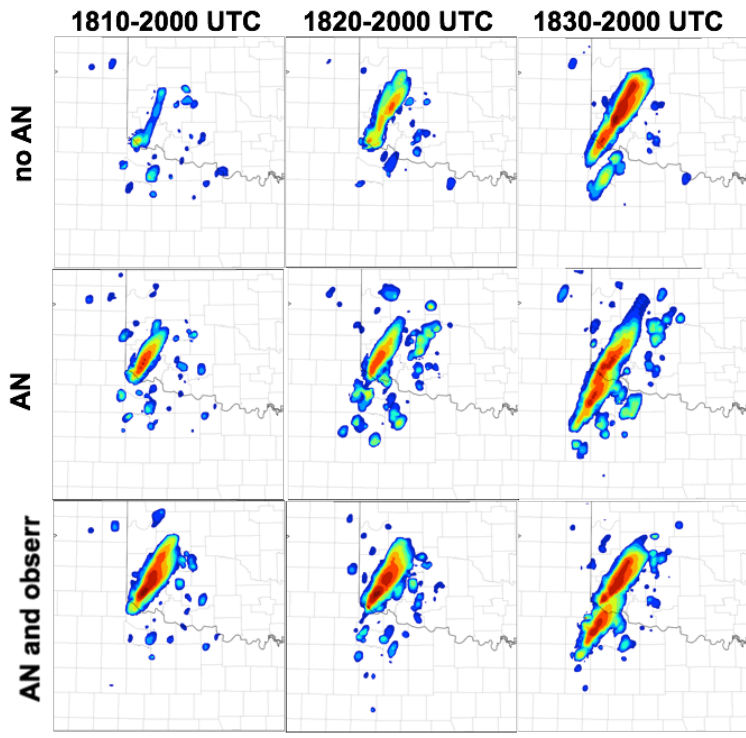


Figure 1. Composite reflectivity swath of forecasts initialized at (left) 1810 UTC, (center) 1820 UTC, and (right) 1830 UTC, for DA configurations with (top) no additive noise, (middle) additive noise, and (bottom) additive noise plus adaptive observation error. Results shown here are for the experiment assimilating radar reflectivity and channel 10 ABI radiance.

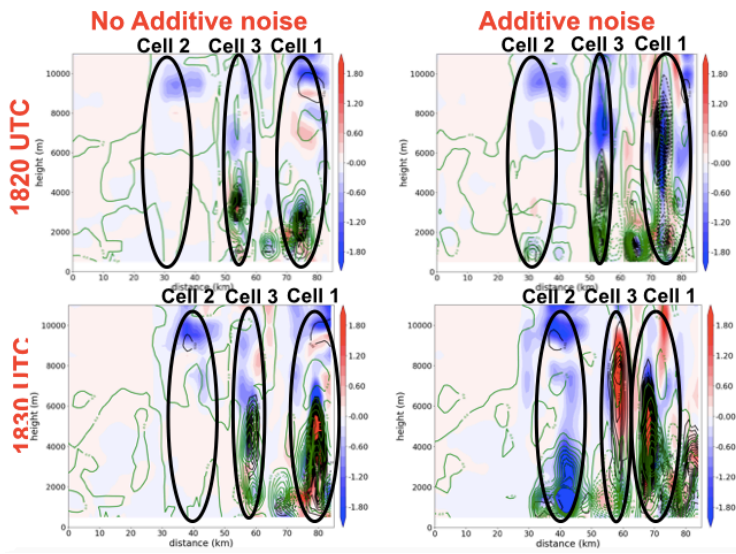


Figure 2. Cross sections of DA increment to potential temperature (shaded), water vapor (green contour), and total cloud hydrometeor (black contour), for (top) the 1820 UTC DA cycle and (bottom) the 1830 UTC DA cycle.

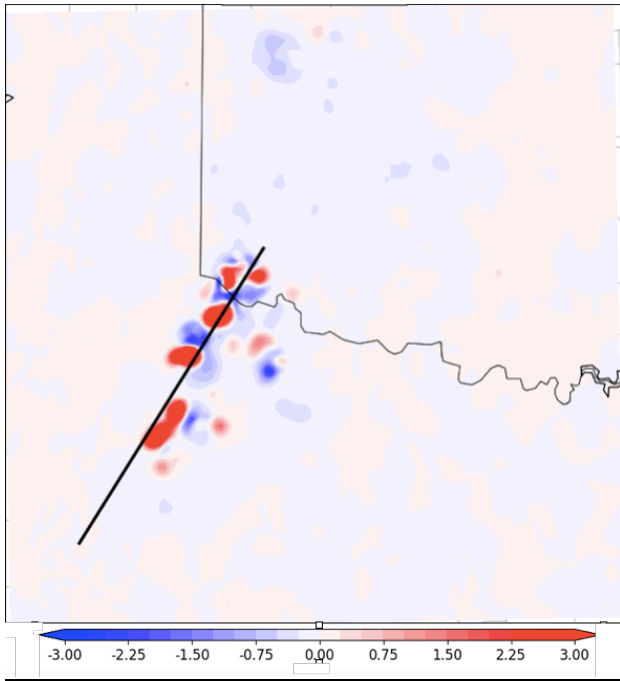


Figure 3. Level 10 (~800 hPa) QVAPOR increment at 1820 UTC (g/kg).

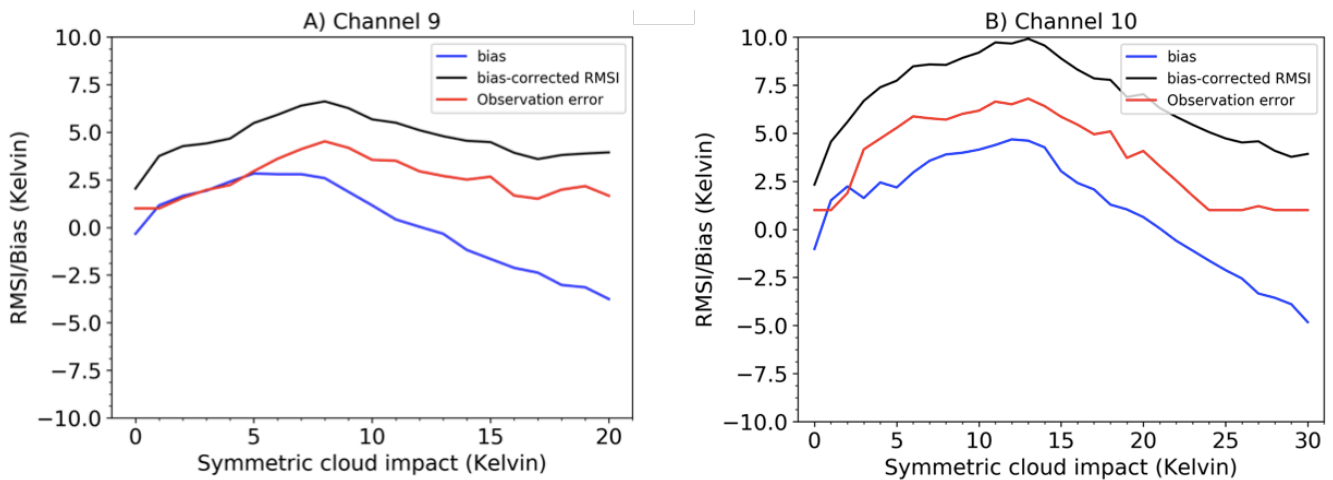


Figure 4. Diagnosed bias (blue line) and bias-corrected RMSE (black line), as well as inferred observation error (red line) as a function of symmetric cloud impact for (a) channel 9 and (b) channel 10.

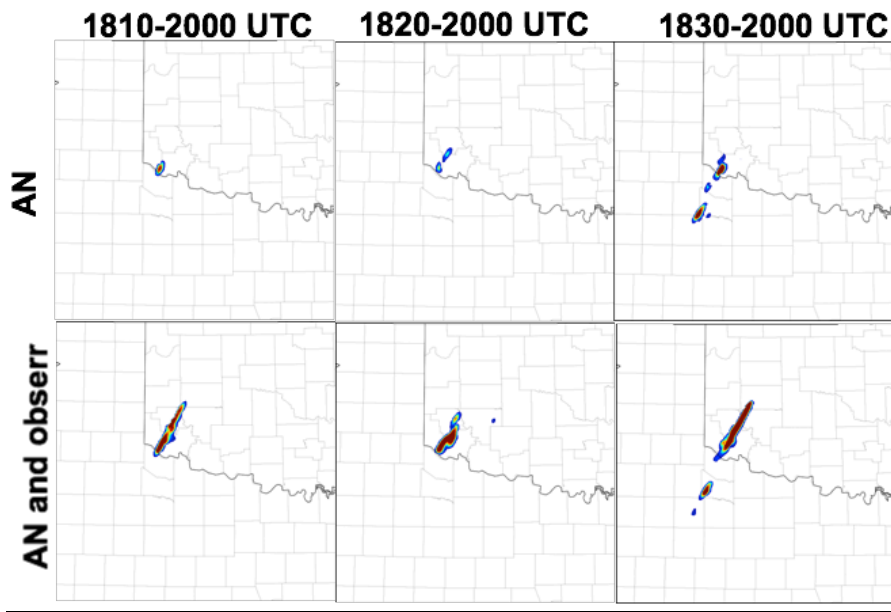


Figure 5. As in the middle and bottom panels of figure 1, except for updraft helicity.

- All experiments used radar DA only from 1610-1700 UTC, 1.1 vertical localization, 15km horizontal, 95% RTPS inflation

Experiment Name	Additive Noise/mask source	ABI Bias Correction	Radar DA	ABI CH9 DA	ABI CH10 DA	ABI Obs. Err.
radaronly	N	---	Y	N	N	---
ch9	N	Cloudy/clear	Y	Y	N	1 K
ch10	N	Cloudy/clear	Y	N	Y	1K
ch9ch10	N	Cloudy/clear	Y	Y	Y	1K
ch9_addn	Y: ch9	Cloudy/clear	Y	Y	N	1K
ch10_addn	Y: ch10	Cloudy/clear	Y	N	Y	1K
Ch9_addn_oberr	Y: ch9	Cloudy/clear	Y	Y	N	adaptive
Ch10_addn_oberr	Y: ch10	Cloudy/clear	Y	N	Y	adaptive
Ch9ch10_addn_oberr	Y: ch9 and ch10	Cloudy/clear	Y	Y	Y	adaptive
Ch9ch10_addn_oberr_bc	Y: ch9 and ch10	adaptive	Y	Y	Y	Adaptive

Table 1. Summary of experiments being included in the manuscript in preparation for Monthly Weather Review.

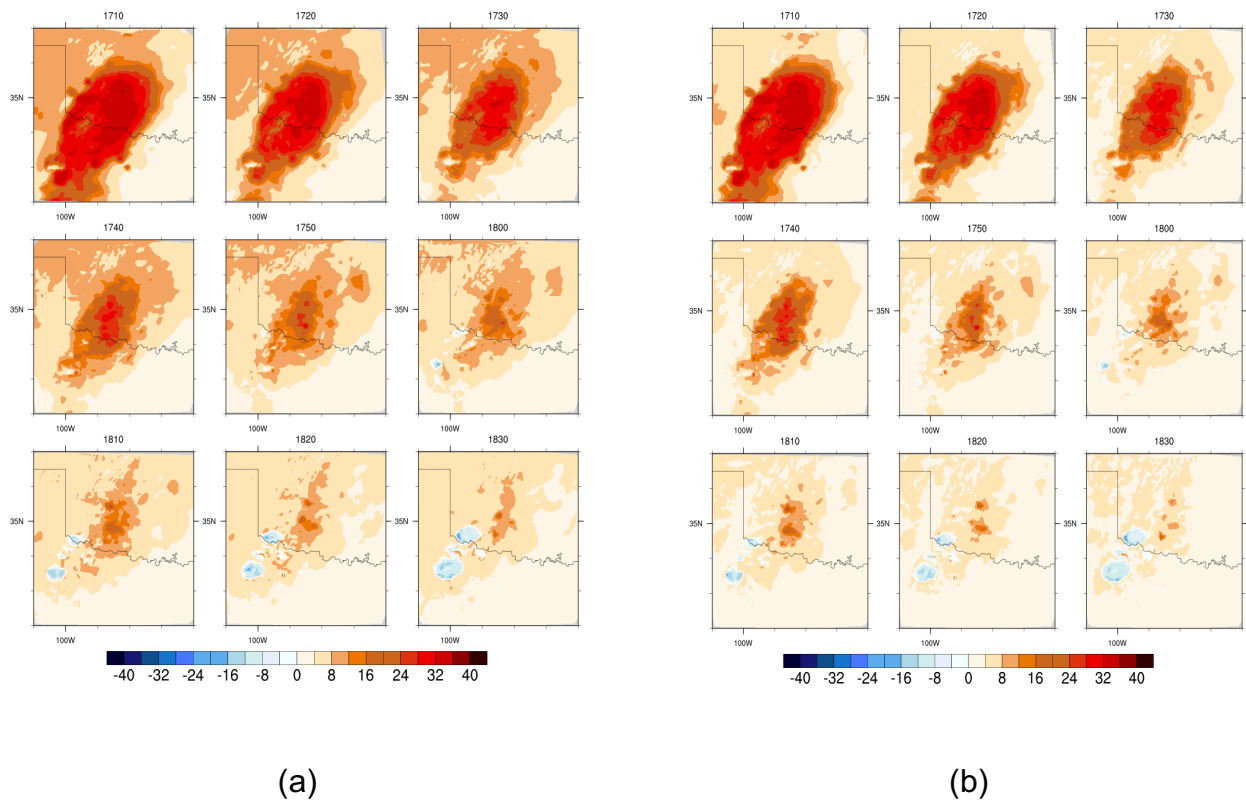


Figure 6: Spatial distribution of observation-minus-analysis (degrees K) from a) offline bias correction and b) online bias correction at different analysis times from 1710 to 1830 UTC.

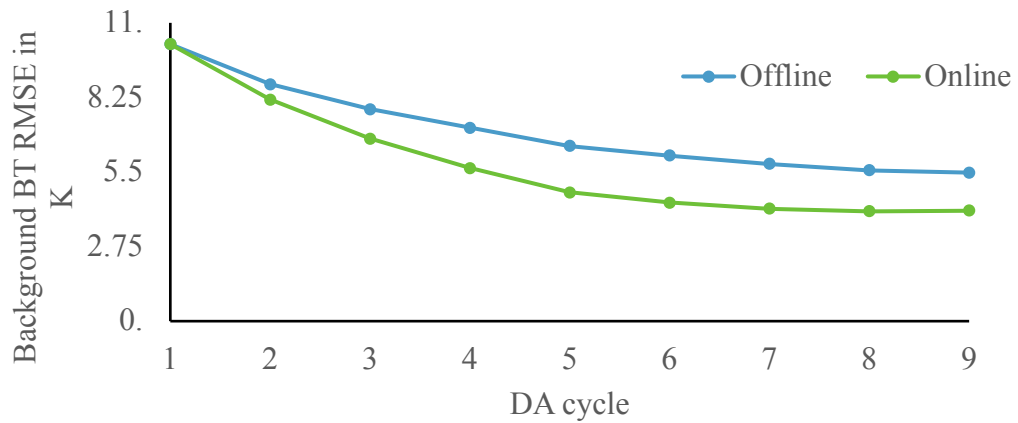


Figure 7: Domain average background brightness temperature RMSE at different DA cycles